

A Stabilizing NMPC Strategy for a Class of Nonholonomic Systems with Drift

Huu Thien Nguyen, Fernando A. C. C. Fontes, and Ionela Prodan

Abstract—In this paper, we present a stabilizing Nonlinear Model Predictive Control (NMPC) scheme tailored for a class of nonholonomic systems with drift, where the acceleration is laterally restrained. Examples include a mobile robot with drifting wheels on a planar surface or a spacecraft maneuvering in a vacuum. The novelty lies in the formulation of the terminal set, reachable from a significant distance from the equilibrium, and the terminal cost, represented as the integration of the stage cost. The proposed approach establishes essential steps for ensuring stability and feasibility guarantees. Simulation results substantiate the viability and effectiveness of the NMPC scheme.

Index Terms—NMPC, nonholonomic system with drift, terminal ingredients.

I. INTRODUCTION

Nonholonomic systems arise frequently in practice, everytime a mechanical device has a constraint on the motion in certain state-space directions [1], examples of which are wheeled vehicles, fixed or rotary-wing aircraft, etc. Prevailing research on nonholonomic systems predominantly revolves around the driftless unicycle model as evidenced by the survey [2]. Regarding a nonholonomic system with drift, the most notable example is a knife-edge moving on a planar plane [3]. A challenging property of nonholonomic systems is the uncontrollability of the linearized dynamics at the origin, which makes it impossible to stabilize them with a continuous feedback controller [4].

NMPC controllers, besides their established ability to manage constraints, are an adequate choice to deal with discontinuous state feedback [5]. Classical techniques to guarantee stability for an NMPC scheme are by using a terminal set constraint, defined as an ellipsoid [6] or a polytope [7], together with a terminal cost, defined as a Lyapunov function of a linearized system. However, these methods require linearization, which makes them an impossible choice to stabilize nonholonomic systems.

Research on NMPC design for nonholonomic systems has delved into various applications, including i) Differential-drive mobile robot and car-like: Worthmann et al. [8] formulate an NMPC for a unicycle mobile robot without terminal

cost nor terminal constraint, where the stability is endorsed with a customized stage cost and a suitable prediction horizon. The differential-drive was also addressed with a stabilizing NMPC in [5, 9] and a robust NMPC in [10]. The car-like was addressed in [11]. ii) Mobile robots with trailers: Rosenfelder et al. [12] design NMPC schemes with kinematics-based non-quadratic costs for stabilizing driftless nonholonomic differential-drive vehicles. iii) Spacecraft attitude: Peterson et al. [13] construct an NMPC scheme for an underactuated spacecraft with two reaction wheels. Their NMPC scheme does not have a terminal cost, but they prove stability with the terminal state constraint equal to zero and the minimum prediction horizon of six steps. iii) Multicopters: a multicopter is classified as a drifting nonholonomic system because, to transition between points in the planar plane or space, the multicopter needs to tilt to orient the thrust generated by its rotors. Subsequently, it tilts in the opposite direction to decelerate. In a specific example, as discussed in [14], an NMPC scheme was introduced with semi-globally asymptotic stability. However, it is important to highlight that this particular approach does not consider rotational dynamics (permitting instantaneous angle changes), and instead, a feedback linearization controller is employed to linearize the multicopter around the equilibrium.

To the best of the authors' knowledge, this is the first work to design a stabilizing NMPC for a class of drift nonholonomic systems with no lateral acceleration.

Notation: Let $\mathbf{0}$ be the zero matrix or vector of appropriate dimension depending on the context, \mathbb{R}^+ be the set of positive real numbers. We denote $\mathbf{x}(t; t_0, \mathbf{x}_{t_0}, \mathbf{u})$ the state \mathbf{x} at time t , starting from $\mathbf{x} = \mathbf{x}_{t_0}$ at $t = t_0$, with the control law \mathbf{u} for $t \geq t_0$. We also use $x_{t_i} \triangleq x(t_i)$ to present the value of the function $x(t)$ at the time index t_i . The outline of the paper is as follows: we first present a spacecraft model, which is a drifting nonholonomic system in Section II. Next, we introduce a terminal set, together with its associated auxiliary controller in Section III. Section IV establishes the NMPC scheme and the main results of the paper, while we demonstrate them through simulations in Section V. Finally, we state the conclusions and suggest some future work in Section VI.

II. SPACECRAFT MODEL

Consider a spacecraft operating in vacuum (with no air resistance and no gravity) as in Fig. 1. The spacecraft is constrained to a plane where it can only move forward, move backward, and rotate around its center of mass by using two bi-directional thrusters. The same model can also represent

This research is supported by FCT/MCTES(PIDDAC), through projects 2020.07959.BD, 2022.02320.PTDC-KEFCODE, and 2022.02801.PTDC-UPWIND-ATOL (<https://doi.org/10.54499/2022.02801.PTDC>).

Huu Thien Nguyen and Fernando A. C. C. Fontes are with SYSTEC-ARISE, University of Porto, Porto, Portugal. huu-thien.nguyen@ieee.org, faf@fe.up.pt

Ionela Prodan is with Univ. Grenoble Alpes, Grenoble INP[†], LCIS, F-26000, Valence, France. ionela.prodan@lcis.grenoble-inp.fr. [†] Institute of Engineering and Management Univ. Grenoble Alpes.

a mobile robot with drifting wheels operating on a slippery plane. We will describe the dynamics of this system and show that it is a nonholonomic system with drift.

We define two coordinate frames, the fixed inertial frame $\mathcal{I} : \{O^{\mathcal{I}}, x^{\mathcal{I}}, z^{\mathcal{I}}\}$ with basis $(e_x^{\mathcal{I}}, e_z^{\mathcal{I}})$, and the body frame $\mathcal{B} : \{O^{\mathcal{B}}, x^{\mathcal{B}}, z^{\mathcal{B}}\}$ whose $O^{\mathcal{B}}$ coincides with the center of mass of the spacecraft, and with the basis $(e_x^{\mathcal{B}}, e_z^{\mathcal{B}})$.

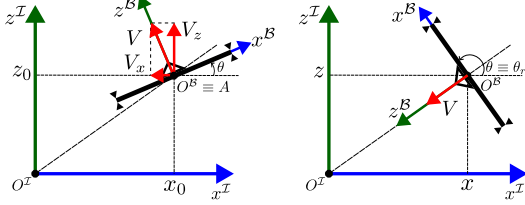


Fig. 1: Spacecraft with an arbitrary pitch angle θ (left) and when its velocity vector \mathbf{V} and its vertical axis $x^{\mathcal{B}}$ point to the origin (right).

The state-space model of the aircraft is:

$$\begin{cases} \dot{x}(t) &= V_x(t), \\ \dot{z}(t) &= V_z(t), \\ \dot{\theta}(t) &= \omega(t), \\ \dot{V}_x(t) &= -a(t) \sin \theta(t), \\ \dot{V}_z(t) &= a(t) \cos \theta(t). \end{cases} \quad (1)$$

Here, the state and control vectors are $\mathbf{x} \triangleq [x, z, \theta, V_x, V_z]^{\top}$, $\mathbf{u} \triangleq [a, \omega]^{\top}$, where x, z are the position of $O^{\mathcal{B}}$ in \mathcal{I} , V_x and V_z are its velocity components in the same inertial frame. We also consider the pitch angle between the body frame $x^{\mathcal{B}}$ axis and the inertial frame $x^{\mathcal{I}}$ axis, i.e., $\theta(t) = \angle(e_x^{\mathcal{B}}, e_x^{\mathcal{I}})$, $\theta(t) \in [-\pi, \pi]$. The control components, ω and a , are the angular speed and the translational acceleration, respectively, with $a(t) \in [-a_m, a_m]$, $\omega(t) \in [-\omega_m, \omega_m]$. The input constraint set is then:

$$\mathcal{U} \triangleq \{\mathbf{u} \in \mathbb{R}^2 \mid -[a_m, \omega_m]^{\top} \leq \mathbf{u} \leq [a_m, \omega_m]^{\top}\}. \quad (2)$$

We define the *displacement vector* $\mathbf{r} \triangleq x(t)e_x^{\mathcal{I}} + z(t)e_z^{\mathcal{I}}$, with $r(t) \triangleq \sqrt{x(t)^2 + z(t)^2}$ being the distance between the spacecraft and the origin. Similarly, we define the *velocity vector* $\mathbf{V} \triangleq V_x(t)e_x^{\mathcal{I}} + V_z(t)e_z^{\mathcal{I}}$, with $V(t) \triangleq \sqrt{V_x(t)^2 + V_z(t)^2}$.

The dynamics (1) are an example of a nonholonomic system with drift [15], which could be written in a compact form as:

$$\dot{\mathbf{x}}(t) = f(\mathbf{x}(t), \mathbf{u}(t)) = f_1(\mathbf{x}(t)) + \sum_{i=1}^2 g_i(\mathbf{x}(t))u_i(t), \quad (3)$$

where the drift term is $f_1(\mathbf{x}(t)) = [V_x(t), V_z(t), 0, 0, 0]^{\top}$, while $g_1(\mathbf{x}(t)) = [0, 0, 0, \sin \theta(t), \cos \theta(t)]^{\top}$, $g_2(\mathbf{x}(t)) = [0, 0, 1, 0, 0]^{\top}$, $u_1(t) = a(t)$, and $u_2(t) = \omega(t)$. Moreover, the dynamics (1) admit a nonholonomic constraint: $\dot{V}_x(t) \cos \theta(t) + \dot{V}_z(t) \sin \theta(t) = 0$, which prevents the spacecraft from accelerating in the $x^{\mathcal{B}}$ direction. As is the case with any nonholonomic system, the linearization of the dynamics (1) at $(\mathbf{x}, \mathbf{u}) = (\mathbf{0}, \mathbf{0})$ is neither controllable nor

stabilizable, which forbids the use of any methods based on linearization, including dual-mode [6] and a vast number of MPC works based on it.

III. AUXILIARY CONTROL STRATEGIES

In this section, we propose a stabilizing strategy for the nominal model. The strategy consists of first driving the state to a set containing the space directions where the nonholonomic systems are easier to stabilize, and then moving to the origin by sliding along this set. Such a process has similarities with sliding mode control, where we first drive the system to a sliding set and then drive the system to the origin along that set. The auxiliary strategy will not necessarily be applied to the system, but will only be used to show that an NMPC scheme is stabilizing. The set mentioned will be the terminal set in the NMPC scheme. This set can be defined to be the set of states with a heading angle pointing towards the origin (see the right side of Fig. 1), from where we can easily reach the origin simply by moving straight on.

Starting from a point A (x_0, z_0) stopped, with $\mathbf{x}_A = [x_0, z_0, 0, 0, 0]^{\top}$, the goal is to move the spacecraft to the equilibrium point $\mathbf{x} = \mathbf{0}$. A possible auxiliary stabilizing strategy (SS) is:

- SS1 Rotate the spacecraft until its vertical axis $z^{\mathcal{B}}$ points to the origin (see Fig. 1).
- SS2 Move forward the target with an acceleration profile $a_{\text{ref}}(t)$ (and consequently with a velocity profile $v_{\text{ref}}(t)$) until reaching the origin of the plane $(x, z) = (0, 0)$.
- SS3 Rotate back to the equilibrium pitch angle $\theta = 0$ and then stop.

To implement this strategy it is convenient to define the *reference pitch angle*, which for any position (x, z) gives the pitch angle that points the thrust to the origin:

$$\theta_r(x, z) = \begin{cases} 0 & \text{if } x = 0, z \leq 0; \\ \pi & \text{if } x = 0, z > 0; \\ \tan^{-1}(-x/z) & \text{if } x \neq 0, z < 0; \\ \pi - \tan^{-1}(x/z) & \text{if } x \neq 0, z > 0; \end{cases} \quad (4)$$

Let us define the *auxiliary controller* that implements the above strategy:

$$\mathbf{u}_{\text{aux}} = [a, \omega]^{\top} = \begin{cases} a = 0, & \omega = -\omega_m & \text{if } \theta > \theta_r; \\ a = 0, & \omega = \omega_m & \text{if } \theta < \theta_r; \\ a = a_r(t), & \omega = 0 & \text{if } \theta = \theta_r, (r, V) \neq \mathbf{0}; \\ a = 0, & \omega = 0 & \text{if } \mathbf{x} = \mathbf{0}; \end{cases} \quad (5)$$

which is equivalent to *Rotate clockwise*, *Rotate anticlockwise*, *Move forward*, and *Stop*. The rotation when $\theta \neq \theta_r$ could be written in the shortened form with the help of the sign function: $\mathbf{u}_{\text{aux}} = [a, \omega]^{\top} = [0, \text{sign}(\theta_r - \theta)\omega_m]^{\top}$ if $\theta \neq \theta_r$. It is clear that the aforementioned control strategy satisfies the input constraint (2). Moreover, it is a discontinuous control law, as expected by Brockett's theorem [4].

The acceleration profile $a_r(t)$ when starting from a stopped position $(V_x, V_z) = (0, 0)$ is (see Fig. 2a):

$$a_r(t) = \begin{cases} a_m & \text{if } t \in [T_0, T_0 + T_1]; & \text{(Accelerate)} \\ -a_m & \text{if } t \in [T_0 + T_1, T_0 + T_2] & \text{(Decelerate)} \end{cases}$$

One of the three cases for the auxiliary stabilizing controller (5) is presented in Fig. 2: i) for $t \in [0, T_0 + T_2]$, the reference pitch angle θ_r is positive. ii) for $t \in [T_0 + T_2, T_0 + T_3]$, when the spacecraft is at the origin, i.e. $(x, z) = (0, 0)$, the reference pitch angle θ_r is 0.

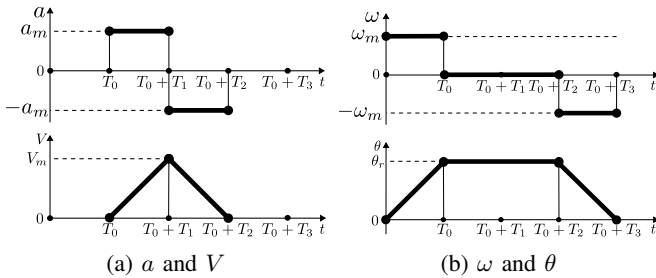


Fig. 2: Proposed auxiliary stabilizing controller and states.

We want the spacecraft to accelerate then decelerate with equal intervals (i.e. $T_2 = 2T_1$), and it travels the distance r_0 from T_0 to $T_0 + T_2$, following the relation $r_0/2 = a_m T_1^2/2$ (see Fig. 2a), which leads to:

$$T_1 = \sqrt{\frac{r_0}{a_m}}, \quad T_2 = 2\sqrt{\frac{r_0}{a_m}}. \quad (6)$$

Regarding the rotations, the rotation from $\theta = 0$ to $\theta = \theta_r$ for $t \in [0, T_0]$ and the rotation from $\theta = \theta_r$ back to $\theta = 0$ for $t \in [T_0 + T_2, T_0 + T_3]$ give:

$$T_0 = \frac{|\theta_r|}{w_m}, \quad T_3 = 2\sqrt{\frac{r_0}{a_m}} + \frac{|\theta_r|}{w_m}. \quad (7)$$

Noting that the spacecraft is symmetrical in the longitudinal axis $\mathbf{x}^{\mathcal{B}}$, we can similarly define a second stabilizing strategy (SS') where the vertical axis $\mathbf{z}^{\mathcal{B}}$ points away from (rather than pointing to) the origin and then the spacecraft moves backward to the origin. The details are in Appendix III.

Next, let us define the *terminal set* to be the set of states for which the spacecraft's vertical axis $\mathbf{z}^{\mathcal{B}}$ points toward (or points away from) the origin and the spacecraft is moving toward (or reversing backward) the origin:

$$\mathcal{X}_f \triangleq \{(x, z, \theta, V_x, V_z) \in \mathbb{R}^2 \times [-\pi, \pi] \times \mathbb{R}^2 \mid \mathbf{r} = -\kappa_1 \mathbf{V} = \kappa_2 \mathbf{e}_z^{\mathcal{B}}, \kappa_1 \in \mathbb{R}^+, \kappa_2 \neq 0, V^2 \leq 2a_m r\}. \quad (8)$$

This set \mathcal{X}_f will serve as terminal region in the NMPC framework. The last condition in the definition of the terminal set imposes that the velocity is sufficiently small so that the spacecraft has room to decelerate and stop at the origin of the plane $(x, z) = (0, 0)$. This is further discussed in Section IV-B.

We can see that with this set definition, the auxiliary strategy (5) makes \mathcal{X}_f invariant with $\kappa_2 < 0$, while the auxiliary strategy SS' makes \mathcal{X}_f invariant with $\kappa_2 > 0$. In this paper, we focus on the analysis of the auxiliary strategy

SS, we also obtain similar results with the auxiliary strategy SS'. The auxiliary strategy SS is equivalently defined as:

- AC1 Rotate to \mathcal{X}_f , i.e. rotate to align the pitch angle $\theta = \theta_r(x, z)$, with the angular rate $\omega = \text{sign}(\theta_r - \theta)w_m$.
- AC2 Move straight to $(x, z) = (0, 0)$ within \mathcal{X}_f following the acceleration profile: $a = a_m$ for $t \in [t_f, t_f + t_1]$ and $a = -a_m$ for $t \in [t_f + t_1, t_f + t_2]$.
- AC3 Rotate to $(x, z, \theta) = (0, 0, 0)$ with the angular rate $\omega = \text{sign}(\theta_r - \theta)w_m = \text{sign}(-\theta)w_m = -\text{sign}(\theta)w_m$ for $t \in [t_f + t_2, t_f + t_3]$ and stop.

The values of t_1 , t_2 , and t_3 are computed in Section IV-A.

Figure 3 shows a snapshot of the spacecraft when it "slides forward" inside the terminal set toward the origin, with the velocity vector \mathbf{V} in red, and the displacement vector \mathbf{r} in brown. Within the terminal set \mathcal{X}_f , we obtain simpler dynamics for the spacecraft defined in (1):

$$\dot{\mathbf{r}}(t) = -\mathbf{V}(t), \quad (9a)$$

$$\dot{\theta}(t) = \omega(t), \quad (9b)$$

$$\dot{V}(t) = a(t), \quad (9c)$$

or, in the compact form with $\mathbf{x}_{ts}(t) = [r(t), \theta(t), V(t)]^\top$ and $\mathbf{u}_{aux}(t)$ as in (5):

$$\dot{\mathbf{x}}_{ts}(t) = f_{ts}(\mathbf{x}_{ts}(t), \mathbf{u}_{aux}(t)). \quad (10)$$

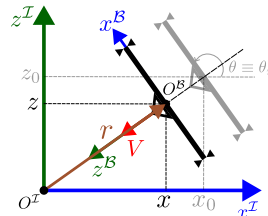


Fig. 3: The spacecraft when it is inside the terminal set \mathcal{X}_f and points to the origin.

IV. NMPC FRAMEWORK

At the time instant t , with the state \mathbf{x}_t , we solve an open-loop optimal control problem (OCP) :

$$\min_{\bar{\mathbf{u}}(\cdot)} J(\bar{\mathbf{x}}, \bar{\mathbf{u}}) = \int_t^{t+T_p} L(\bar{\mathbf{x}}(\tau), \bar{\mathbf{u}}(\tau)) d\tau + F(\bar{\mathbf{x}}(t+T_p)), \quad (11)$$

$$\text{subject to: } \dot{\bar{\mathbf{x}}}(\tau) = f(\bar{\mathbf{x}}(\tau), \bar{\mathbf{u}}(\tau)), \quad \tau \in [t, t+T_p] \quad (12a)$$

$$\bar{\mathbf{u}}(\tau) \in \mathcal{U}, \quad \tau \in [t, t+T_p] \quad (12b)$$

$$\bar{\mathbf{x}}(t) = \mathbf{x}_t, \quad (12c)$$

$$\bar{\mathbf{x}}(t+T_p) \in \mathcal{X}_f. \quad (12d)$$

Here $\bar{\mathbf{x}}(\tau) = \mathbf{x}(\tau; t, \mathbf{x}_t, \bar{\mathbf{u}})$ is the predicted state at the time τ , starting from \mathbf{x}_t at t , under the predicted control input $\bar{\mathbf{u}}$, which is the optimal solution to the OCP. The set \mathcal{U} is input constraint set in (2), \mathcal{X}_f is terminal set defined in (8), and T_p is the prediction horizon. The first part of the solution, $\bar{\mathbf{u}}(\tau), \tau \in [t, t+\delta]$, is applied to the system, then the time shifts $t \leftarrow t + \delta$, and the problem (11)–(12) is

solved repeatedly. The MPC law $\mathbf{u}^*(\cdot)$ is constructed by the concatenation of the solutions of (11)–(12) that are applied to the system [11, 16].

We define respectively the stage cost L and the terminal cost F in (11) as follows:

$$L(\mathbf{x}_\tau, \mathbf{u}_\tau) = x_\tau^2 + z_\tau^2 + V_{x_\tau}^2 + V_{z_\tau}^2 + \theta_\tau^2, \quad (13a)$$

$$F(\mathbf{x}_{t_f}) = \int_{t_f}^{\infty} L(\bar{\mathbf{x}}(\tau; t_f, \mathbf{x}_{t_f}, \mathbf{u}_{\text{aux}}), \mathbf{u}_{\text{aux}}(\tau)) d\tau. \quad (13b)$$

The terminal cost defined this way is guaranteed to be finite and can be explicitly computed since the auxiliary controller drives the state to the origin in finite time.

We provide in Algorithm 1 the steps to design an NMPC controller with guaranteed stability.

Algorithm 1 NMPC for a drifting nonholonomic vehicle in the planar plane with laterally restricted acceleration

data The dynamics f in (3), the initial state \mathbf{x}_0 , the acceleration and angular velocity limits a_m, ω_m , the error tolerance ϵ_r .

- 1: Define the MPC design parameters $(L, F, T_p, \mathcal{X}_f)$ satisfying the stability conditions SC1–SC5 defined below.
 - 2: Set the time $t = 0$.
 - 3: **while** $r^2 \geq \epsilon_r$ **do**
 - 4: Obtain the current state \mathbf{x}_t .
 - 5: Solve the OCP (11)–(12).
 - 6: Assign the first segment of the optimal input, $\bar{\mathbf{u}}(\tau), \tau \in [t, t + \delta]$ to $\mathbf{u}^*(\cdot)$ and apply it to the plant.
 - 7: Shift the time $t \leftarrow t + \delta$.
 - 8: **end while**
- result** NMPC law $\mathbf{u}^*(\cdot)$
-

A. Explicit expression for the terminal cost

Figure 4 presents the concept of the auxiliary controller inside an NMPC iteration when $\theta_{t_f} > 0$. After the time stamp t_f , the auxiliary controller \mathbf{u}_{aux} , which is never applied to the system, is used to compute the terminal cost F and verify the stability conditions. For $t \in [t_f, t_f + t_1]$, $\mathbf{u}_{\text{aux}} = [a_m, 0]^\top$ to accelerate the spacecraft to its maximum velocity V_m , then for $t \in [t_f + t_1, t_f + t_2]$, $\mathbf{u}_{\text{aux}} = [-a_m, 0]^\top$ to decelerate the spacecraft to zero velocity. Finally, for $t \in [t_f + t_2, t_f + t_3]$, $\mathbf{u}_{\text{aux}} = [0, \text{sign}(\theta_r - \theta_{t_f})\omega_m]^\top = [0, \text{sign}(-\theta_{t_f})\omega_m]^\top = [0, -\text{sign}(\theta_{t_f})\omega_m]^\top$ to rotate the spacecraft's pitch angle from θ_{t_f} to 0. The time stamps t_1, t_2 , and t_3 are chosen such that, the velocity V and the distance r at $t_f + t_2$ are 0, while from $t_f + t_2$ to $t_f + t_3$, the pitch angle goes from θ_{t_f} to 0.

Lemma 4.1: The time stamps t_1, t_2 , and t_3 in the auxiliary strategy AC2–AC3 when starting from $(r, V) = (r_{t_f}, V_{t_f})$ are calculated as follows:

$$t_1 = -\frac{V_{t_f}}{a_m} + \frac{\sqrt{V_{t_f}^2 + 2a_m r_{t_f}}}{a_m \sqrt{2}}, \quad (14a)$$

$$t_2 = -\frac{V_{t_f}}{a_m} + \frac{\sqrt{2}\sqrt{V_{t_f}^2 + 2a_m r_{t_f}}}{a_m}, \quad (14b)$$

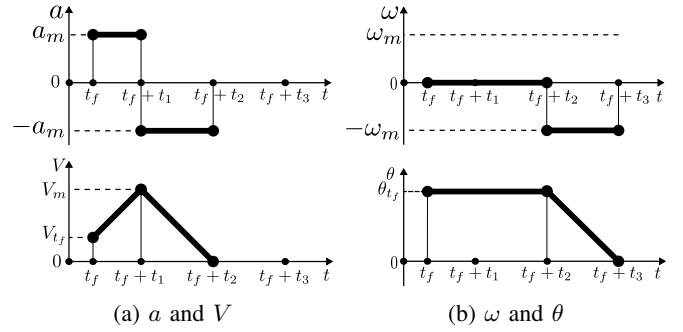


Fig. 4: The auxiliary stabilizing controller AC and states inside the terminal set.

$$t_3 = \frac{|\theta_{t_f}|}{\omega_m} - \frac{V_{t_f}}{a_m} + \frac{\sqrt{2}\sqrt{V_{t_f}^2 + 2a_m r_{t_f}}}{a_m}. \quad (14c)$$

Proof: The proof is in Appendix I. \square

Remark 1: The time stamps t_2 and t_3 are always non-negative. Hence, the time stamp t_1 is non-negative when:

$$V_{x_{t_f}}^2 + V_{z_{t_f}}^2 \leq 2a_m \sqrt{x_{t_f}^2 + z_{t_f}^2}, \quad (15)$$

which explains the last condition in (8).

Inside the terminal set, with the state variables $\mathbf{x}_{ts}(t) = [r(t), \theta(t), V(t)]^\top$ in (10), we write the stage cost (13a) as:

$$L(\bar{\mathbf{x}}(\tau), \bar{\mathbf{u}}(\tau)) = x(\tau)^2 + z(\tau)^2 + V_x(\tau)^2 + V_z(\tau)^2 + \theta(\tau)^2 = r(\tau)^2 + V(\tau)^2 + \theta(\tau)^2. \quad (16)$$

Using this new stage cost, with the auxiliary controller AC2–AC3, we derive the exact formula for the terminal cost (13b).

Proposition 4.2: The explicit value of the terminal cost is:

$$F(\mathbf{x}) = \theta^2 \left(\frac{\sqrt{2}\sqrt{V^2 + 2a_m r} - V}{a_m} \right) + \frac{1}{3} \frac{|\theta^3|}{\omega_m} + \frac{\sqrt{2}(V^2 + 2a_m r)^{3/2}(23V^2 + 40a_m^2 + 46a_m r)}{240a_m^3} - \left(\frac{1}{3} \frac{V^3}{a_m} + \frac{Vr^2}{a_m} + \frac{2}{3} \frac{V^3 r}{a_m^2} + \frac{2}{15} \frac{V^5}{a_m^3} \right), \quad (17)$$

with $V = \sqrt{V_x^2 + V_z^2}$ and $r = \sqrt{x^2 + z^2}$.

Proof: The proof is in Appendix I. \square

B. Stability analysis

For the NMPC algorithm 1, with prediction horizon T_p , stage cost L as in (13a), terminal cost F as in (13b), and the terminal set \mathcal{X}_f , stability can be guaranteed if these design parameters are chosen satisfying the following five stability conditions. [11]

- SC1 The terminal set \mathcal{X}_f is closed and contains the origin.
- SC2 The stage cost L is continuous and positive definite.
- SC3 The terminal cost F is positive semi-definite and continuously differentiable.
- SC4 \mathcal{X}_f is reachable in the prediction horizon T_p from any initial states.

SC5 For all $t^* \in [t_f, \infty)$ and for all $\mathbf{x}_t \in \mathcal{X}_f$, there exists a $\delta > 0$ such that the control function $\mathbf{u}_{\text{aux}} : [t^*, t^* + \delta] \rightarrow \mathbb{R}^2$, verifies $\mathbf{u}_{\text{aux}} \in \mathcal{U}$, makes the terminal set \mathcal{X}_f invariant, and satisfies:

$$\frac{dF(\mathbf{x}(t; t^*, \mathbf{x}_t, \mathbf{u}_{\text{aux}}))}{dt} \leq -L(\mathbf{x}(t; t^*, \mathbf{x}_t, \mathbf{u}_{\text{aux}})). \quad (18)$$

Theorem 4.3: Since the model (1) satisfies assumptions H1–H4 in [11], the chosen design parameters T_p , L , F , and \mathcal{X}_f satisfy the stability conditions SC1–SC5, the NMPC scheme of Algorithm 1 is stabilizing.

Proof: The model clearly satisfies H1–H4 in [11] since \mathcal{U} is bounded and $f(0,0) = 0$. The conditions SC1–SC2 can be easily verified. From the definition of F in (13b), and SC2, F is clearly positive semi-definite, and its time derivative is continuous, so SC3 is satisfied. For SC4, the spacecraft can rotate to the terminal set \mathcal{X}_f with the maximum angle of π . We provide here a sketch of the proof for the last condition SC5, showing that $\dot{F}(\mathbf{x}(t; t_f, \mathbf{x}_{t_f}, \mathbf{u}_{\text{aux}})) = -L(\mathbf{x}(t; t_f, \mathbf{x}_{t_f}, \mathbf{u}_{\text{aux}}))$. By employing the dynamics inside the terminal set as in (10), the time derivative of the terminal cost (17) is:

$$\begin{aligned} \frac{dF(\mathbf{x}(t; t_f, \mathbf{x}_{t_f}, \mathbf{u}_{\text{aux}}))}{dt} &= \frac{\partial F(\mathbf{x}(t))}{\partial \mathbf{x}_{ts}} \cdot \frac{d\mathbf{x}_{ts}(t)}{dt} \\ &= \nabla_{\mathbf{x}_{ts}} F(\mathbf{x}(t)) \cdot f_{ts}(\mathbf{x}_{ts}(t), \mathbf{u}_{\text{aux}}(t)) \end{aligned} \quad (19)$$

with the auxiliary controller as in AC2–AC3, but instead of using the time dependence, we utilize the state dependence:

$$\mathbf{u}_{\text{aux}} = [a, \omega]^\top = \begin{cases} [a_m, 0]^\top & \triangleq \mathbf{1} \mathbf{u}_{\text{aux}} \text{ if } (r, V) \neq \mathbf{0}, V^2 < 2a_m r \\ [-a_m, 0]^\top & \triangleq \mathbf{2} \mathbf{u}_{\text{aux}} \text{ if } (r, V) \neq \mathbf{0}, V^2 = 2a_m r \\ [0, -\text{sign}(\theta)w_m]^\top & \triangleq \mathbf{3} \mathbf{u}_{\text{aux}} \text{ if } (r, V) = \mathbf{0}, \end{cases}$$

which implies *Accelerate*, *Decelerate*, and *Rotate at origin* inside the terminal set \mathcal{X}_f .

The explicit equations for the partial derivative $\nabla_{\mathbf{x}_{ts}} F(\mathbf{x}(t))$ and the time derivative $\dot{F}(\mathbf{x}(t; t_f, \mathbf{x}_{t_f}, \mathbf{u}_{\text{aux}}))$ when $(r, V) \neq \mathbf{0}$ are in Appendix II. If $(r, V) = \mathbf{0}$, the terminal cost (17) and its partial derivative are:

$$F(\mathbf{x}) = \frac{1}{3} \frac{|\theta^3|}{\omega_m}, \quad \nabla_{\mathbf{x}_{ts}} F(\mathbf{x}(t)) = \frac{\text{sign}(\theta)\theta^2}{\omega_m}. \quad (20)$$

We now check three cases, which are equivalent to the three cases of the auxiliary controller.

$$1) \mathbf{u}_{\text{aux}} = \mathbf{1} \mathbf{u}_{\text{aux}} = [a_m, 0]^\top, (r, V) \neq \mathbf{0}, V^2 < 2a_m r:$$

$$\frac{dF(\mathbf{x}(t; t_f, \mathbf{x}_{t_f}, \mathbf{1} \mathbf{u}_{\text{aux}}))}{dt} = -(r^2 + \theta^2 + V^2). \quad (21)$$

$$2) \mathbf{u}_{\text{aux}} = \mathbf{2} \mathbf{u}_{\text{aux}} = [-a_m, 0]^\top, (r, V) \neq \mathbf{0}, V^2 = 2a_m r:$$

$$\frac{dF(\mathbf{x}(t; t_f, \mathbf{x}_{t_f}, \mathbf{2} \mathbf{u}_{\text{aux}}))}{dt} = -(r^2 + \theta^2 + V^2). \quad (22)$$

$$3) \mathbf{u}_{\text{aux}} = \mathbf{3} \mathbf{u}_{\text{aux}} = [0, -\text{sign}(\theta)\omega_m]^\top, (r, V) = \mathbf{0}:$$

$$\frac{dF(\mathbf{x}(t; t_f, \mathbf{x}_{t_f}, \mathbf{3} \mathbf{u}_{\text{aux}}))}{dt} = -\text{sign}^2(\theta)\theta^2 = -\theta^2. \quad (23)$$

Eqns. (21)–(23) satisfy SC5, thus, completing the proof. \square

V. SIMULATIONS

To validate the NMPC controller in Algorithm 1, we test it on a spacecraft with the following input constraints:

$$\mathcal{U} \triangleq \{\mathbf{u} \in \mathbb{R}^2 \mid -[\sqrt{2}, \pi/8]^\top \leq \mathbf{u} \leq [\sqrt{2}, \pi/8]^\top\}. \quad (24)$$

The function $\theta_r(x, z)$ in (4) is conveniently implemented in MATLAB or Python with the command $\theta_r(x, z) = \text{atan2}(x, -z)$. We first run a forward simulation with the controller (5), then simulate NMPC controllers.

A. Initial forward simulation

We first simulate the motion of the spacecraft from the initial point $\mathbf{x}_A = [-4, 4, 0, 0, 0, 0]^\top$ to the point $\mathbf{x} = \mathbf{0}$ using the auxiliary control law (5). The dynamics (1) is discretized using the Runge-Kutta 4th order method with the step size $h = 0.1$, we choose the MPC sampling time to be $\delta = 0.1s$. The simulation results are in Fig. 5.

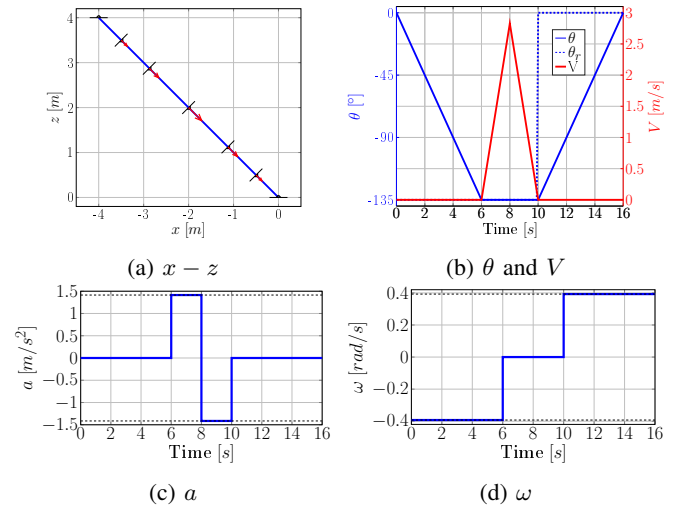


Fig. 5: Simulation results for the spacecraft with the auxiliary controller, starting at $(x_0, z_0) = (-4, 4)$.

The reference pitch angle θ_r following (4) is $-3\pi/4$ (rad), so the spacecraft takes $(-3\pi/4)/(-\pi/8) = 6s$ to align $z^{\mathcal{B}}$ pointing to the origin. Next, using (6), $T_1 = T_2 = 2s$. Finally, employing (5), the rotation to $\theta = 0$ at $(x, z) = (0, 0)$ takes $\frac{\text{sign}(-(-3\pi/4))}{\pi/8} = 6s$ to complete.

B. NMPC simulation

For the NMPC simulation, we want to stabilize the spacecraft also from the initial state $\mathbf{x}_A = [-4, 4, 0, 0, 0, 0]^\top$. We choose prediction horizon to be $T_p = \left\lfloor \frac{\pi}{\omega_m \delta} \right\rfloor + 1 = 61$ (steps). The OCP (11)–(12) is solved using the Direct Multiple Shooting technique [17], the dynamics (1) are discretized using the Runge-Kutta 4th order method with the step size $h = 0.1$. We choose the error tolerance ϵ_r in Algorithm 1, line 3 to be $\epsilon_r = 10^{-8}$.

The simulation is done in MATLAB R2023a, using the CasADi toolbox [18] with IPOPT solver [19]. We formulate

the terminal set constraint (8) on vector directions using the dot product and the cross product:

$$\mathbf{V}_{t_f} \times \mathbf{e}_z^B = 0, \quad (25a)$$

$$\mathbf{r}_{t_f} \times \mathbf{e}_z^B = 0, \quad (25b)$$

$$\mathbf{r}_{t_f} \cdot \mathbf{V}_{t_f} = -\|\mathbf{r}_{t_f}\| \|\mathbf{V}_{t_f}\|. \quad (25c)$$

These constraints are implemented numerically as $(1 - \epsilon_f)\|\mathbf{V}_{t_f}\| \leq (-V_{x_{t_f}} \sin \theta_{t_f} + V_{z_{t_f}} \cos \theta_{t_f}) \leq \|\mathbf{V}_{t_f}\|$, $-\|\mathbf{r}_{t_f}\| \leq (-x_{t_f} \sin \theta_{t_f} + z_{t_f} \cos \theta_{t_f})^2 \leq (-1 + \epsilon_f)\|\mathbf{r}_{t_f}\|$, $-\|\mathbf{V}_{t_f}\| \|\mathbf{r}_{t_f}\| \leq (V_{x_{t_f}} z_{t_f} + V_{z_{t_f}} x_{t_f})^2 \leq (-1 + \epsilon_f)\|\mathbf{V}_{t_f}\| \|\mathbf{r}_{t_f}\|$, with $\epsilon_f = 0$. We use a solution of the forward simulation, where the spacecraft is first inside the terminal set (i.e., when the pitch angle equals the reference pitch angle) as the initial guess for the first NMPC iteration. Other NMPC iterations use the warm-start method from the solution of the previous iteration. We choose the sampling time $\delta = 0.1s$. The simulation results are in Figs. 6a–7.

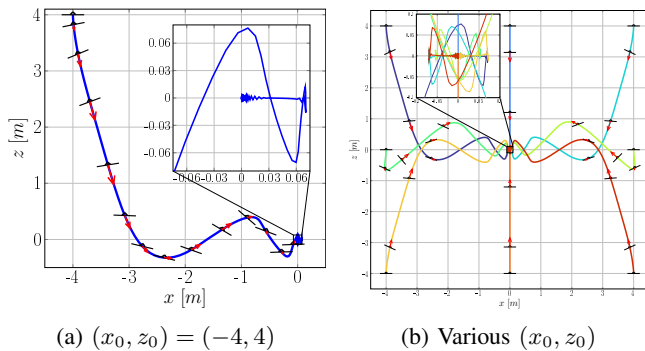


Fig. 6: Spacecraft $x - z$ trajectory.

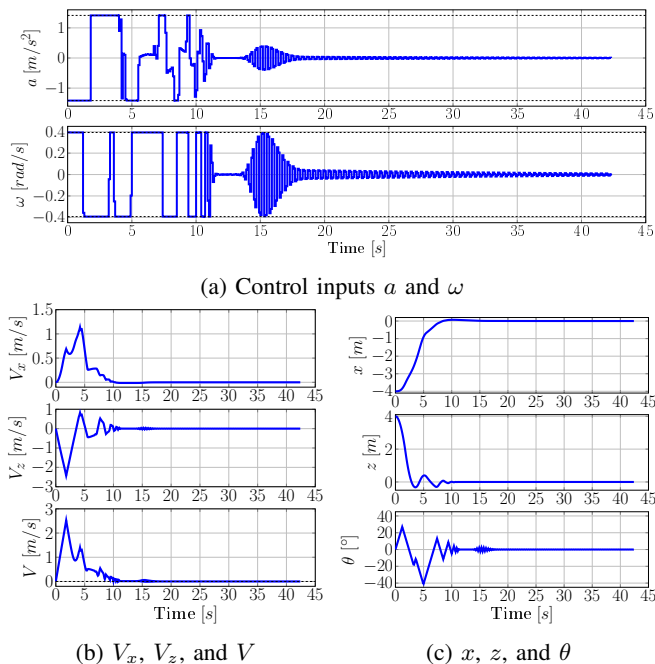


Fig. 7: Simulation results for the spacecraft with the NMPC controller, starting at $(x_0, z_0) = (-4, 4)$.

The control inputs a and ω are in Fig. 7a, satisfying the input constraints (24). In Figure 6a, we see that the spacecraft approaches the origin from the right, with the pitch angle θ chattering around 0° (Fig. 7c). Since the spacecraft has no lateral acceleration, it executes damped oscillations around its center of mass by attenuating the angular rate ω (Fig. 7a). All the five states of the spacecraft are converging to 0, which illustrates the stability of the proposed NMPC scheme.

Figure 6b shows the $x - z$ trajectory of the spacecraft for $(x_0, z_0) \in \{-4, 0, 4\} \times \{-4, 0, 4\} \setminus (0, 0)$. An interesting observation is the spacecraft executes the final damping maneuvers on the half plane $x \geq 0$ or $x \leq 0$ that is the opposite of the other half-plane in which it started at x_0 .

VI. CONCLUSIONS AND FUTURE WORKS

This paper presents an NMPC scheme for a class of drift nonholonomic systems with lateral acceleration restrained, where the terminal set is a region of a subspace, which contains the modes where the nonholonomic system is easily controllable. For future work, we will investigate how to implement a similar technique to amulticopter, which is another drifting nonholonomic system.

REFERENCES

- [1] I. Kolmanovsky and N. McClamroch, "Developments in nonholonomic control problems," *IEEE Control Systems Magazine*, vol. 15, no. 6, pp. 20–36, Dec. 1995.
- [2] T. P. Nascimento, C. E. T. Dórea, and L. M. G. Gonçalves, "Nonholonomic mobile robots' trajectory tracking model predictive control: A survey," *Robotica*, vol. 36, no. 5, pp. 676–696, May 2018.
- [3] A. Bloch and M. Reyhanoglu, "Controllability and stabilizability properties of a nonholonomic control system," in *29th IEEE Conference on Decision and Control*. Honolulu, HI, USA: IEEE, 1990, pp. 1312–1314 vol.3.
- [4] R. W. Brockett, "Asymptotic stability and feedback stabilization," *Differential geometric control theory*, vol. 27, no. 1, pp. 181–191, 1983.
- [5] F. A. C. C. Fontes, "Discontinuous feedbacks, discontinuous optimal controls, and continuous-time model predictive control," *Int. J. Robust Nonlinear Control*, vol. 13, no. 3–4, pp. 191–209, Mar. 2003.
- [6] H. Chen and F. Allgöwer, "A quasi-infinite horizon nonlinear model predictive control scheme with guaranteed stability," *Automatica*, vol. 34, no. 10, pp. 1205–1217, 1998.
- [7] M. Cannon, V. Deshmukh, and B. Kouvaritakis, "Nonlinear model predictive control with polytopic invariant sets," *Automatica*, vol. 39, no. 8, pp. 1487–1494, Aug. 2003.
- [8] K. Worthmann, M. W. Mehrez, M. Zanon, G. K. I. Mann, R. G. Gosine, and M. Diehl, "Model Predictive Control of Nonholonomic Mobile Robots Without Stabilizing Constraints and Costs," *IEEE Trans. Contr. Syst. Technol.*, vol. 24, no. 4, pp. 1394–1406, July 2016.
- [9] Dongbing Gu and Huosheng Hu, "A stabilizing receding horizon regulator for nonholonomic mobile robots," *IEEE Trans. Robot.*, vol. 21, no. 5, pp. 1022–1028, Oct. 2005.
- [10] F. Fontes and L. Magni, "Min-max model predictive control of nonlinear systems using discontinuous feedbacks," *IEEE Trans. Automat. Contr.*, vol. 48, no. 10, pp. 1750–1755, Oct. 2003.
- [11] F. A. Fontes, "A general framework to design stabilizing nonlinear model predictive controllers," *Systems & Control Letters*, vol. 42, no. 2, pp. 127–143, Feb. 2001.
- [12] M. Rosenfelder, H. Ebel, J. Krauspenhaar, and P. Eberhard, "Model predictive control of non-holonomic systems: Beyond differential-drive vehicles," *Automatica*, vol. 152, p. 110972, June 2023.
- [13] C. D. Petersen, F. Leve, and I. Kolmanovsky, "Model Predictive Control of an Underactuated Spacecraft with Two Reaction Wheels," *J. Guid. Control Dyn.*, vol. 40, no. 2, pp. 320–332, Feb. 2017.
- [14] H. T. Nguyen, N. T. Nguyen, and I. Prodan, "Notes on the terminal region enlargement of a stabilizing NMPC design for a multicopter," *Automatica*, vol. 159, p. 111375, Jan. 2024.

- [15] J.-M. Godhavn, A. Balluchi, L. Crawford, and S. Sastry, "Steering of a class of nonholonomic systems with drift terms," *Automatica*, vol. 35, no. 5, pp. 837–847, May 1999.
- [16] L. Grüne and J. Pannek, *Nonlinear Model Predictive Control*, ser. Communications and Control Engineering. Cham: Springer International Publishing, 2017.
- [17] H. Bock and K. Plitt, "A Multiple Shooting Algorithm for Direct Solution of Optimal Control Problems," *IFAC Proceedings Volumes*, vol. 17, no. 2, pp. 1603–1608, July 1984.
- [18] J. A. E. Andersson, J. Gillis, G. Horn, J. B. Rawlings, and M. Diehl, "CasADi: A software framework for nonlinear optimization and optimal control," *Math. Prog. Comp.*, vol. 11, no. 1, pp. 1–36, Mar. 2019.
- [19] A. Wächter and L. T. Biegler, "On the implementation of an interior-point filter line-search algorithm for large-scale nonlinear programming," *Math. Program.*, vol. 106, no. 1, pp. 25–57, Mar. 2006.

APPENDIX I

STEPS TO CALCULATE THE TERMINAL COST

We decompose the terminal cost (13b) into four terms, which are equivalent to the time intervals $\tau \in [t_f, t_f + t_1]$, $\tau \in [t_f + t_1, t_f + t_2]$, $\tau \in [t_f + t_2, t_f + t_3]$, and $\tau \in [t_f + t_3, \infty]$, and we respectively denote each term as F_1 , F_2 , F_3 , and F_4 :

$$F((\bar{\mathbf{x}}(t_f))) = \underbrace{\int_{t_f}^{t_f+t_1} L((\bar{\mathbf{x}}(\tau))d\tau}_{F_1} + \underbrace{\int_{t_f+t_1}^{t_f+t_2} L((\bar{\mathbf{x}}(\tau))d\tau}_{F_2} \\ + \underbrace{\int_{t_f+t_2}^{t_f+t_3} L((\bar{\mathbf{x}}(\tau))d\tau}_{F_3} + \underbrace{\int_{t_f+t_3}^{\infty} L((\bar{\mathbf{x}}(\tau))d\tau}_{F_4}.$$

We now proceed to calculate the explicit values of F_1 , F_2 , F_3 , F_4 , and the terminal cost F .

The velocity at $t_f + t_1$, which we call the maximum velocity V_m , is:

$$V_m = V_{t_f} + \int_{t_f}^{t_f+t_1} a(\tau)d\tau = V_{t_f} + a_m t_1.$$

From $t_f + t_1$ to $t_f + t_2$, by looking at the Fig. 4a, we can obtain the relation between t_2 and t_1 as follows

$$t_2 - t_1 = \frac{V_m}{a_m} = \frac{V_{t_f} + a_m t_1}{a_m} \Rightarrow t_2 = 2t_1 + \frac{V_{t_f}}{a_m}. \quad (26)$$

We want at $t_f + t_2$, the distance $r(t_f + t_2)$ is 0, which means the area of below the function $V(t)$ over t as in Fig. 4a, equals to r_{t_f} :

$$r_{t_f} = \frac{1}{2}(V_{t_f} + V_m)t_1 + \frac{1}{2}V_m(t_2 - t_1) \\ = \frac{1}{2} \left(4V_{t_f}t_1 + 2a_m t_1^2 + \frac{V_{t_f}^2}{a_m} \right) \\ = 2V_{t_f}t_1 + a_m t_1^2 + \frac{V_{t_f}^2}{2a_m}. \quad (27)$$

Rewriting the terms of (27) and solving for t_1 , we obtain:

$$a_m t_1^2 + 2V_{t_f}t_1 + \left(\frac{V_{t_f}^2}{2a_m} - r_{t_f} \right) = 0, \quad (28)$$

with $\Delta = (2V_{t_f})^2 - 4(a_m)\left(\frac{V_{t_f}^2}{2a_m} - r_{t_f}\right) = 2(V_{t_f}^2 + 2a_m r_{t_f})$. Since $V_{t_f} \geq 0$, $a_m \geq 0$, and $r_{t_f} \geq 0$, which lead to $\Delta \geq 0$, hence (28) always has at least one solution.

By solving (28), combing with (26), the explicit formulas for t_1 and t_2 are:

$$t_1 = -\frac{V_{t_f}}{a_m} + \frac{\sqrt{V_{t_f}^2 + 2a_m r_{t_f}}}{a_m \sqrt{2}}, \quad (29a)$$

$$t_2 = -\frac{V_{t_f}}{a_m} + \frac{\sqrt{2}\sqrt{V_{t_f}^2 + 2a_m r_{t_f}}}{a_m}. \quad (29b)$$

Remark 2: Note that, to make the auxiliary controller valid, i.e. we want the spacecraft to accelerate then decelerate

inside the terminal set \mathcal{X}_f , we must have the condition $t_1 \geq 0$, which is equivalent to the condition:

$$V_{x_{t_f}}^2 + V_{z_{t_f}}^2 \leq 2a_m \sqrt{x_{t_f}^2 + z_{t_f}^2}. \quad (30)$$

For $t \in [t_f, t_f + t_1]$, with the acceleration $a(t) = a_m$ and the pitch angle $\theta(t) = \theta_{t_f} = \theta_r$, the velocity and the distance of the spacecraft to the origin are:

$$V(t) = V_{t_f} + \int_{t_f}^t a(\tau)d\tau = V_{t_f} + \int_{t_f}^t (a_m)d\tau \\ = V_{t_f} + a_m(t - t_f),$$

$$r(t) = r_{t_f} - \int_{t_f}^t V(\tau)d\tau = r_{t_f} - \int_{t_f}^t [V_{t_f} + a_m(\tau - t_f)]d\tau \\ = r_{t_f} - V_{t_f}(t - t_f) - \frac{a_m}{2}(t - t_f)^2.$$

The first terminal cost term F_1 is now calculated as

$$F_1 = \int_{t_f}^{t_f+t_1} (r(\tau)^2 + V(\tau)^2 + \theta(\tau)^2)d\tau \\ = \theta_{t_f}^2 t_1 + \int_{t_f}^{t_f+t_1} \left\{ [r_{t_f} - V_{t_f}(\tau - t_f) - \frac{a_m}{2}(\tau - t_f)^2]^2 \right. \\ \left. + [V_{t_f} + a_m(\tau - t_f)]^2 \right\} d\tau \\ = (\theta_{t_f}^2 + r_{t_f}^2 + V_{t_f}^2)t_1 - V_{t_f}(r_{t_f} - a_m)t_1^2 \\ + \frac{1}{3}(V_{t_f}^2 + a_m^2 - a_m r_{t_f})t_1^3 + \frac{1}{4}a_m V_{t_f}t_1^4 + \frac{1}{20}a_m^2 t_1^5.$$

At $t = t_f + t_1$, the velocity and the distance are

$$V(t_f + t_1) = V_{t_f} + a_m t_1, \\ r(t_f + t_1) = r_{t_f} - V_{t_f}t_1 - \frac{a_m}{2}t_1^2.$$

For $t \in [t_f + t_1, t_f + t_2]$, with the acceleration $a(t) = -a_m$ and the pitch angle $\theta(t) = \theta_{t_f} = \theta_r$, the velocity and the distance of the spacecraft to the origin are:

$$V(t) = V(t_f + t_1) + \int_{t_f+t_1}^t a(\tau)d\tau \\ = V_{t_f} + a_m t_1 - a_m(t - t_f - t_1) \\ = V_{t_f} - a_m(t - t_f - 2t_1),$$

$$r(t) = r(t_f + t_1) - \int_{t_f+t_1}^t V(\tau)d\tau \\ = r(t_f + t_1) - \int_{t_f+t_1}^t [V_{t_f} - a_m(\tau - t_f - 2t_1)]d\tau \\ = \left(r_{t_f} - V_{t_f}t_1 - \frac{a_m}{2}t_1^2 \right) - V_{t_f}(t - t_f - t_1) \\ + \frac{a_m}{2}(t - t_f - 2t_1)^2 - \frac{a_m}{2}t_1^2 \\ = r_{t_f} - V_{t_f}(t - t_f) - a_m t_1^2 + \frac{a_m}{2}(t - t_f - 2t_1)^2.$$

The second terminal cost term F_2 is in (32).

For $t \in [t_f + t_2, t_f + t_3]$, the spacecraft rotates back to $\theta = 0$ from θ_{t_f} , where the pitch angle and the needed for

$$\begin{aligned}
F_2 &= \int_{t_f+t_1}^{t_f+t_2} (r(\tau)^2 + V(\tau)^2 + \theta(\tau)^2) d\tau \\
&= \theta_{t_f}^2 (t_2 - t_1) + \int_{t_f+t_1}^{t_f+t_2} \left\{ \left[r_{t_f} - V_{t_f}(\tau - t_f) - a_m t_1^2 + \frac{a_m}{2}(\tau - t_f - 2t_1)^2 \right]^2 + \left[V_{t_f} - a_m(\tau - t_f - 2t_1) \right]^2 \right\} d\tau \\
&= \theta_{t_f}^2 (t_2 - t_1) + \frac{1}{3} (t_2 - t_1) \left\{ \left[\frac{13t_1^4}{20} - \frac{47t_2 t_1^3}{20} + \left(\frac{73t_2^2}{20} + 7 \right) t_1^2 + \left(-\frac{27}{20} t_2^3 - 5t_2 \right) t_1 + \frac{3t_2^4}{20} + t_2^2 \right] a_m^2 \right. \\
&\quad + \left[\frac{V_{t_f} t_1^3}{4} + \left[\frac{V_{t_f} t_2}{4} + r_{t_f} \right] t_1^2 + \left[\frac{13}{4} V_{t_f} t_2^2 - 5r_{t_f} t_2 + 9V_{t_f} \right] t_1 - \frac{3V_{t_f} t_2^3}{4} + r_{t_f} t_2^2 - 3V_{t_f} t_2 \right] a_m \\
&\quad \left. + V_{t_f}^2 t_1^2 + V_{t_f} [V_{t_f} t_2 - 3r_{t_f}] t_1 + V_{t_f}^2 t_2^2 - 3V_{t_f} r_{t_f} t_2 + 3V_{t_f}^2 + 3r_{t_f}^2 \right\}. \tag{32}
\end{aligned}$$

the rotation are:

$$\theta(t) = \theta_{t_f} - \text{sign}(\theta_{t_f}) \omega_m (t - t_f - t_2), \tag{33a}$$

$$t_3 - t_2 = \frac{|\theta_{t_f}|}{\omega_m}. \tag{33b}$$

Therefore, the terminal cost term for the rotation back to $\theta = 0$ from $\theta = \theta_{t_f}$ at the origin $(x, z) = (0, 0)$ is:

$$\begin{aligned}
F_3 &= \int_{t_f+t_2}^{t_f+t_3} [\theta_{t_f}^2 - 2\theta_{t_f} \text{sign}(\theta_{t_f}) \omega_m (t - t_f - t_2) \\
&\quad + (\text{sign}(\theta_{t_f}) \omega_m (t - t_f - t_2))^2] dt = \frac{1}{3} \frac{|\theta_{t_f}^3|}{\omega_m}. \tag{34}
\end{aligned}$$

When $t \in [t + t_4, \infty]$, all the states are zeros (i.e. $\mathbf{x} = \mathbf{0}$), therefore,

$$F_4 = 0. \tag{35}$$

Finally, the terminal cost is presented in (36), which completes the proof.

$$\begin{aligned}
F(\mathbf{x}_{t_f}) &= F_1 + F_2 + F_3 + F_4 \\
&= \theta_{t_f}^2 \left(-\frac{V_{t_f}}{a_m} + \frac{\sqrt{2} \sqrt{V_{t_f}^2 + 2a_m r_{t_f}}}{a_m} \right) + \frac{1}{3} \frac{|\theta_{t_f}^3|}{\omega_m} \\
&\quad + \frac{\sqrt{2} (V_{t_f}^2 + 2a_m r_{t_f})^{3/2} (23V_{t_f}^2 + 40a_m^2 + 46a_m r_{t_f})}{240a_m^3} \\
&\quad - \left(\frac{1}{3} \frac{V_{t_f}^3}{a_m} + \frac{V_{t_f} r_{t_f}^2}{a_m} + \frac{2}{3} \frac{V_{t_f}^3 r_{t_f}}{a_m^2} + \frac{2}{15} \frac{V_{t_f}^5}{a_m^3} \right). \tag{36}
\end{aligned}$$

APPENDIX II

EXPLICIT TIME DERIVATIVE OF THE TERMINAL COST

The explicit equation for the partial derivative $\nabla_{\mathbf{x}_{ts}} F(\mathbf{x}(t))$ and the time derivative $\dot{F}(\mathbf{x}(t); t_f, \mathbf{x}_{t_f}, \mathbf{u}_{\text{aux}})$ when $(r, V) \neq \mathbf{0}$ are in (37) and (38).

APPENDIX III

AUXILIARY CONTROLLER ANALYSIS WHEN THE SPACECRAFT POINTING AWAY FROM THE ORIGIN

This appendix presents briefly the results when we use the stabilizing strategy SS' where the vertical axis $z^{\mathcal{B}}$ points away from (rather than pointing to) the origin and then the spacecraft moves backwards to the origin.

The second stabilizing strategy SS' is defined as follows:

SS'1 Rotate the spacecraft so that its vertical axis $z^{\mathcal{B}}$ points away from the origin .

SS'2 Move *backwards* the target with an acceleration profile $a'_{\text{ref}}(t)$ until reaching the origin of the plane $(x, z) = (0, 0)$.

SS'3 Rotate back to $\theta = 0$ and then stop.

With this strategy, the reference pitch is $\theta'_r(x, z) = \theta_r(x, z) - \pi$, and the second auxiliary controller is:

$$\begin{aligned}
\mathbf{u}'_{\text{aux}} &= [a, \omega]^T = \\
&\begin{cases} a = 0, & \omega = -\omega_m & \text{if } \theta > \theta'_r; \\ a = 0, & \omega = \omega_m & \text{if } \theta < \theta'_r; \\ a = a'_r(t), & \omega = 0 & \text{if } \theta = \theta'_r, (r, V) \neq \mathbf{0}; \\ a = 0, & \omega = 0 & \text{if } \mathbf{x} = \mathbf{0}; \end{cases} \tag{39}
\end{aligned}$$

with the acceleration profile:

$$a'_r(t) = \begin{cases} -a_m & \text{if } t \in [T_0, T_0 + T_1] & \text{(Decelerate)} \\ a_m & \text{if } t \in [T_0 + T_1, T_0 + T_2] & \text{(Accelerate)} \end{cases}$$

The auxiliary strategy SS' is equivalently defined as:

AC'1 Rotate to \mathcal{X}_f , i.e. rotate to align the pitch angle $\theta = \theta'_r(x, z)$, with the angular rate $\omega = \text{sign}(\theta'_r - \theta) \omega_m$.

AC'2 Reverse straight to $(x, z) = (0, 0)$ within \mathcal{X}_f following the acceleration profile: $a = -a_m$ for $t \in [t_f, t_f + t_1]$ and $a = a_m$ for $t \in [t_f + t_1, t_f + t_2]$.

AC'3 Rotate to $(x, z, \theta) = (0, 0, 0)$ with the angular rate $\omega = -\text{sign}(\theta) \omega_m$ for $t \in [t_f + t_2, t_f + t_3]$ and stop.

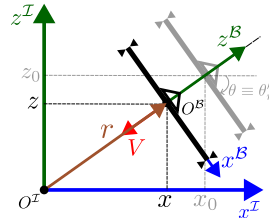


Fig. 8: The spacecraft when it is inside the terminal set \mathcal{X}_f and points away from origin.

Figure 8 shows a snapshot of the spacecraft when it “reverses” inside the terminal set backward the origin, with the velocity vector V in red, and the displacement vector

If $(r, V) \neq \mathbf{0}$:

$$\nabla_{\mathbf{x}_{ts}} F(\mathbf{x}(t)) = \begin{bmatrix} \frac{23\sqrt{2}\sigma_2^{3/2}}{120a_m^2} - \frac{2V^3}{3a_m^2} + \frac{\sqrt{2}\theta^2}{\sqrt{\sigma_2}} - \frac{2Vr}{a_m} + \frac{\sqrt{2}\sqrt{\sigma_2}\sigma_1}{80a_m^2} \\ \frac{\text{sign}(\theta)\theta^2}{w_m} - 2\theta \left(\frac{V}{a_m} - \frac{\sqrt{2}\sqrt{\sigma_2}}{a_m} \right) \\ \frac{23\sqrt{2}V\sigma_2^{3/2}}{120a_m^3} - \frac{V^2}{a_m} - \frac{2V^4}{3a_m^3} - \frac{r^2}{a_m} - \frac{2V^2r}{a_m^2} - \theta^2 \left(\frac{\sqrt{\sigma_2} - \sqrt{2}V}{a_m\sqrt{\sigma_2}} \right) + \frac{\sqrt{2}V\sqrt{\sigma_2}\sigma_1}{80a_m^3} \end{bmatrix}, \quad (37)$$

with $\sigma_1 = 23V^2 + 40a_m^2 + 46ra_m$, and $\sigma_2 = V^2 + 2a_mr$.

$$\begin{aligned} \frac{dF(\mathbf{x}(t; t_f, \mathbf{x}_{t_f}, \mathbf{u}_{\text{aux}}))}{dt} &= \nabla_{\mathbf{x}_{ts}} F(\mathbf{x}(t)) \cdot f_{ts}(\mathbf{x}_{ts}(t), \mathbf{u}_{\text{aux}}(t)) \\ &= -V \left(\frac{23\sqrt{2}\sigma_2^{3/2}}{120a_m^2} - \frac{2V^3}{3a_m^2} + \frac{\sqrt{2}\theta^2}{\sqrt{\sigma_2}} - \frac{2Vr}{a_m} + \frac{\sqrt{2}\sqrt{\sigma_2}\sigma_1}{80a_m^2} \right) \\ &\quad + \omega \left[\frac{\text{sign}(\theta)\theta^2}{w_m} - 2\theta \left(\frac{V}{a_m} - \frac{\sqrt{2}\sqrt{\sigma_2}}{a_m} \right) \right] \\ &\quad + a \left[\frac{23\sqrt{2}V\sigma_2^{3/2}}{120a_m^3} - \frac{V^2}{a_m} - \frac{2V^4}{3a_m^3} - \frac{r^2}{a_m} - \frac{2V^2r}{a_m^2} - \theta^2 \left(\frac{\sqrt{\sigma_2} - \sqrt{2}V}{a_m\sqrt{\sigma_2}} \right) + \frac{\sqrt{2}V\sqrt{\sigma_2}\sigma_1}{80a_m^3} \right]. \end{aligned} \quad (38)$$

r in brown. Within the terminal set \mathcal{X}_f , we obtain simpler dynamics for the spacecraft defined in (1):

$$\dot{r}(t) = V(t), \quad (40a)$$

$$\dot{\theta}(t) = \omega(t), \quad (40b)$$

$$\dot{V}(t) = a(t), \quad (40c)$$

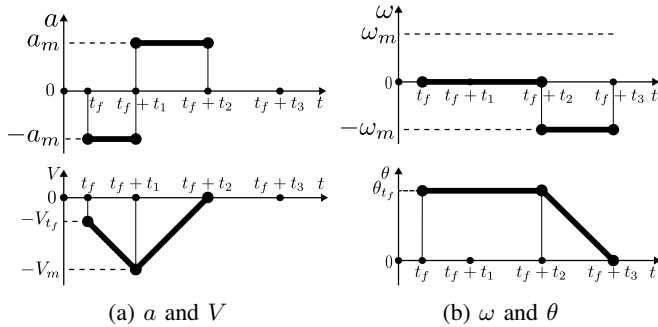


Fig. 9: The auxiliary stabilizing controller AC' and states inside the terminal set.

The difference lies in Fig. 9a, where algebraic value of the velocity vector V is negative since the spacecraft is reversing in its body frame.

The Lemma 4.1 and Proposition 4.2 also hold with this auxiliary strategy, therefore, the Theorem 4.3 holds.